Light-off Investigation of Oxymethylene Ether (OME) Considering the Presence of the Exhaust Components Heptane, Carbon, and Nitrogen Monoxide

Florian Rümmele[1] [ORCID] · **Alexander Susdorf**[1] · **Syed Muhammad Salman Haider**[1] · **Robert Szolak**[1]

Abstract

Synthetic fuels and fuel blends like OMEs can contribute to tank-to-wheel CO_2 emission savings. At the same time, it is known that these fuels have a lower exhaust temperature compared to conventional diesel. This effect has major impact on the exhaust after-treatment system, particularly in cold start conditions. This paper investigates the light-off behavior of exhaust gases containing OMEs by temperature-programmed oxidation experiments using a state-of-the-art oxidation catalyst. The main side product of catalytic oxidation of OMEs between 100 °C and the oxidation temperature T_{50}, which was around 160 °C, was shown to be formaldehyde. While alkane oxidation, in this case heptane, was little influenced by OME oxidation, the oxidation temperature T_{50} of CO increases by more than 10 °C by OME addition. Nitrogen monoxide impeded the oxidation of OME in a similar way to the other components investigated. Due to the amount of FA produced and its toxicity, it could be concluded that it is necessary to heat up exhaust after-treatment systems of OME diesel engines even faster than conventional diesel exhaust after-treatment systems. The relatively high reactivity of OME on oxidation catalyst can be used by active thermal management approaches.

Keywords Synthetic fuel · OME · Light-off · Temperature-programmed oxidation · Oxidation catalyst · CatVap · Active thermal management

Abbreviations

OME	Oxymethylene ether
C_7	Heptane
NO_x	Nitrogen oxides
SCR	Selective catalytic reduction
GHSV	Gas hourly space velocity
FTIR	Fourier transform infrared spectrometer
ICE	Internal combustion engine
MFC	Mass flow controller
EH	Electric heater
H_2	Hydrogen
CO	Carbon monoxide
CO_2	Carbon dioxide
NO	Nitrogen monoxide
$T_{50,i}$	Temperature at which 50% conversion efficiency of component i has been reached
TPO	Temperature-programmed oxidation
TPL	Thymolphthalein
FA	Formaldehyde
WHTC	World Harmonized Transient Cycle

✉ Florian Rümmele
 florian.ruemmele@ise.fraunhofer.de

1 Fraunhofer Institute for Solar Energy Systems ISE, Freiburg, Germany

1 Introduction

In accordance with climate protection targets for greenhouse gas emissions, vehicle fleet operators and freight companies are looking to increase engine efficiency. One way for engine manufacturers to do this is to increase the thermodynamic efficiency of modern diesel engines by improving the turbomachinery and the combustion parameters such as increased compression ratio and peak in-cylinder pressures [1]. These efficiency improvements contribute to fuel savings and tank-to-wheel carbon dioxide (CO_2) emission savings by decreasing the exhaust energy, i.e., the exhaust temperature of the engine. To comply with the new emission limitations, it is mandatory that moderate temperature levels be reached quickly for selective catalytic reduction (SCR) of nitrogen oxides (NO_x) with NH_3 in the case of lean combustion [2]. In experimental investigations

with a 7-l Euro 5 engine, Bai et al. found that the exhaust temperature is lower than 200 °C for over half of the driving cycle in the cold start World Harmonized Transient Cycle (WHTC) without control strategies of exhaust thermal management [3]. Investigations with passenger cars in the challenging Transport for London (TfL) driving cycle show also that during half of the driving cycle, low exhaust temperatures hinder reliable NO_x conversion via SCR technology [4]. An LNT (Lean NO_x Trap) is used along with a dual-dosing SCR system combined with internal combustion measures like Miller cycles and air-exhaust path management via flaps to reach NO_x emissions as set down by the Euro 6d requirements under real driving conditions. Investigations show that high engine efficiency resulted in exhaust temperatures, which are too low to prevent NO_x, hydrocarbon (HC), and carbon monoxide (CO) emissions [5, 6]. Especially with respect to the new legislation with highly dynamic driving requirements, internal and external thermal management measures are essential in order to quickly reach the temperatures required by the catalytic after-treatment.

Oxidation catalysts are an integral component in exhaust after-treatment systems of combustion engines. They oxidize pollutants, like HC and CO, in the exhaust gas, to unreactive CO_2, thereby generating heat. Nitrogen monoxide is known to hinder the oxidation of gaseous carbon species by blocking catalyst surface sites and therefore increases the oxidation and light-off temperature of exhaust gas mixtures [7]. The extent of inhibition is related to the amount of adsorbed nitrogen oxide, and the increase of oxidation temperature was up to 30 °C higher relative to that of a pre-reduced and pre-oxidized catalyst [7]. Furthermore, oxidation catalysts are used to form nitrogen dioxide (NO_2) from nitrogen monoxide and oxygen. The presence of NO_2 is advantageous and enables the so-called fast SCR reaction, converting an equimolar amount of NO and NO_2. This reaction enhances the reaction rate at temperatures below 300 °C compared to SCR reaction with NO solely [8].

The catalyst performance is highly dependent on its light-off behavior. An important key parameter for catalytic oxidation of fuels is the oxidation or light-off temperature. In this paper, $T_{50,i}$ is defined as the temperature at which 50% conversion efficiency of component i is reached [9]. Once the oxidation catalyst has reached its light-off temperature (T_{50}), it can be used for heating up the off-gas. This is generally done by dosing fuel via late injection in the cylinder or at the metering unit between the engine and the oxidation catalyst. The heat is needed to eliminate NO_x by SCR technology in low load operation as mentioned previously.

Synthetic fuels and fuel blends are also currently being investigated to assess the further reduction potential of the well-to-wheel emissions. Oxymethylene ethers (OMEs) are a promising alternative for diesel fuel since they can be blended into diesel. This gives them a major advantage over gaseous e-fuels for global distribution [10]. Though OMEs have lower energy densities than diesel (around half the energy density

based on weight), process pathways to produce OMEs from renewable electricity and electrolysis exist with 86% less well-to-wheel CO_2 emissions compared to fossil diesel fuel [11]. The formation of OME is a chain reaction of formaldehyde (FA), which is why synthesized OME is present as a mixture of components with various chain lengths. From synthesis, OME is known to be reactive at temperatures even below 50 °C in the presence of a catalyst [10]. Due to the high toxicity of FA, it is particularly important to suppress its back-reactions from OME to FA. As in OME synthesis, the decomposition has many side products, like methyl formate, formic acid, CO, methanol, and dimethyl ether. The role of water, which is present in the engine exhaust gas, has been emphasized in synthesis and decomposition many times [12]. Investigations on burning OME and OME blends in slightly modified lean combustion engines have been performed intensively [13–16]. It was concluded that replacing diesel with OME leads to a strong reduction of particle emissions. A particle filter is though indispensable because of particle number limitations [17]. Willems et al. found that OME combustion leads to lower exhaust temperatures, which prevents the catalyst light-off [15]. Therefore and because of the beforementioned increase of engine efficiency, the behavior (reactivity, secondary products) of OME and OME blends on oxidation catalysts in cold start condition is important to analyze for emission control and future exhaust after-treatment systems.

Based on its reactivity at low temperatures, OME could form different reaction products whose absorption properties and whose interaction with other exhaust gas components on the catalyst are largely unknown. In exhaust catalyst science, extensive studies concerning the concurrence between hydrocarbon and NO_x on precious metal catalyst have been carried out [7, 18, 19]. To the best of the author's knowledge, there is still uncertainty about the light-off behavior of OME on oxidation catalysts in the presence of other exhaust components like heptane (C_7) and nitrogen and carbon oxides.

The knowledge acquired from this work will contribute light-off data for the simulation of exhaust after-treatment systems of engines operated with OME. Catalyst composition, size, and heat-up strategies can be developed to reduce the known emissions as well as the secondary emissions from OME. A new, renewable fuel will only find social acceptance if it can be burned without emitting toxic pollutants or strong greenhouse gases.

2 Experimental

2.1 Test Rig for Temperature-Programmed Oxidation

The test rig used in the experiments was self-manufactured at Fraunhofer ISE to simulate the exhaust gases of internal

combustion engines (ICE). The schematic diagram of the test rig for temperature-programmed oxidation (TPO) experiments is shown in Fig. 1. The following components could be mixed and supplied individually:

- Air, CO, CO_2, and nitrogen monoxide (NO) supplied by the mass flow controllers
- OME supplied through a NE-300 KF technology microsyringe pump, passed through an evaporator with nitrogen (N_2) as a carrier
- Water and heptane (surrogate for diesel) supplied from two saturator tanks with air and N_2 as carriers respectively. At high temperatures, the gases were oversaturated and then cooled down to a defined concentration.

The components are brought together in the hot mixing zone installed inside an oven. Here, they are mixed evenly and heated to a uniform temperature before reaching the oxidation reactor. The oven is equipped with electric heaters (EH) and a fan to ensure homogenous heat distribution throughout its volume and in the hot mixing zone. An additional heater is used for the saturation of gas streams with water and heptane respectively. A cooler is installed with each saturation tank to lower the temperature to attain the desired water and heptane concentration respectively.

For analyzing the composition of the feed streams with a Fourier transform infrared spectrometer (FTIR) of the Type 2030 Multi-Gas Analyzer, it was possible to bypass the reactor via a fast switching three-way valve.

2.2 Oxidation Catalyst and Reactor

An aged oxidation catalyst provided by FEV Europe was mounted inside a quartz glass reactor as shown in Fig. 2. The catalyst washcoat composition and cell density are equivalent to ceramic catalysts used in series automobile diesel Euro 6 applications with state-of-the-art precious metal content. The temperature of the catalyst can be controlled by a heater and the reactor was insulated with a glass wool material. The catalyst temperature was constantly recorded with a thermocouple placed in the middle of the catalyst, and with the heater individual temperature ramps can be realized. In all experiments, a ramp of 5 °C per minute was used. The exhaust gas enters the reactor through the inlet, passes over the catalyst where the oxidation takes place, and departs from the outlet towards FTIR. The gas hourly space velocity (GHSV) of approximately 60,000 l/h, which can be described as the ratio of the flow rate of the feed-in gas at norm conditions (273 K and 1 atm) to the volume of the catalyst bed, can be found in exhaust after-treatment literature
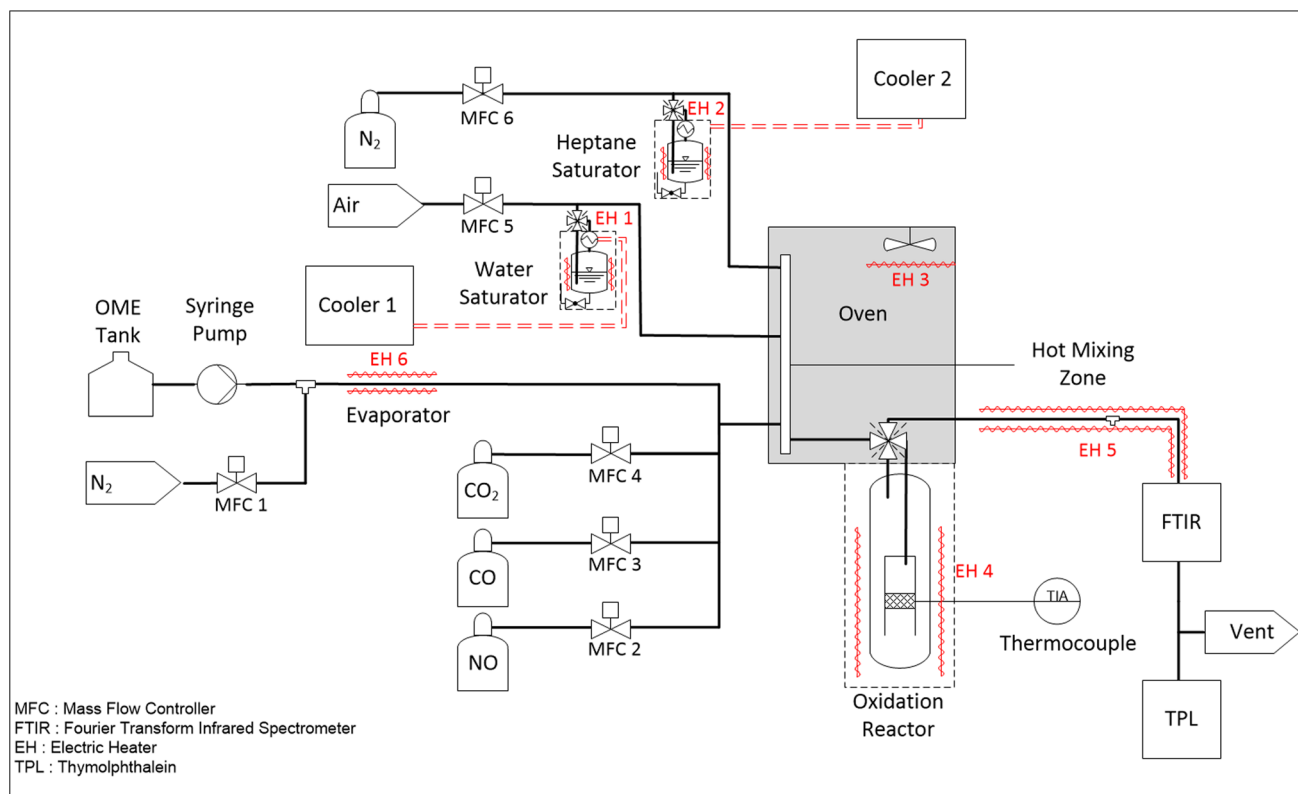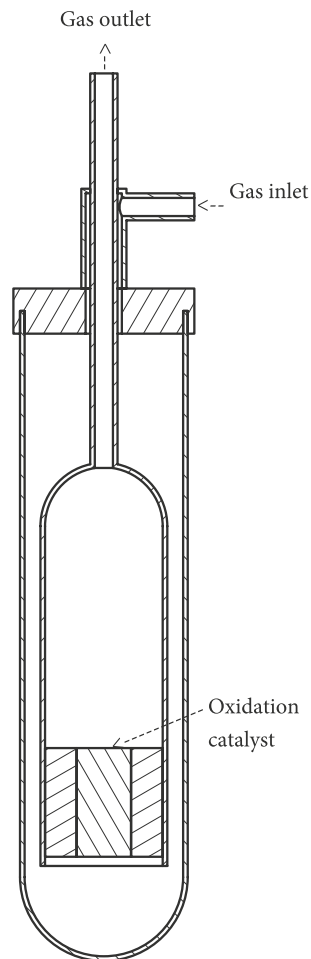

Fig. 1 Simplified process flow chart of the test rig at Fraunhofer ISE

Fig. 2 The oxidation reactor with a catalyst bed of 4.8 cm^3 is feed the 4.8 l_N/min (GHSV = 60,000 h^{-1})

Gas outlet

Gas inlet

Oxidation catalyst

frequently and was set via the mass flow controllers (MFCs) of the feed gas [20, 21].

2.3 Experimental Procedure

The typical diesel engine off-gas used comprised 10% O_2, 7.4% H_2O, and 7% CO_2 concentration by volume. The same exhaust composition was used in all the experiments, unless stated otherwise. In all experiments, the gases sum up to a volume flow of 4.8 l_N/min. After flowing through the oxidation catalyst, the gas from the reactor is fed into FTIR

downstream, which recorded the spectrums of individual components for qualitative and quantitative analyses.

Since the concentrations of all exhaust components vary greatly in dynamic engine operation, different concentrations of CO, NO, heptane, and OME were tested. Common CO and HC, represented by heptane exhaust concentrations for a state-of-the-art lean diesel passenger car engines, were tested [22].

The molecular formula of OME can be described as $H_3CO–(CH_2O)_n–CH_3$ where n describes the length of chain [23]. The OME, mainly consisting of OME_3 to OME_5, was supplied and analyzed with gas chromatographic and oscillation (DIN 12,185) methods by ASG Analytics. Based on the analysis of the mixture, the resulting molecular formula was $H_3CO–(CH_2O)_{3.5}–CH_3$ with the mean molar mass of 150.7 mol/g. Table 1 is a list of relevant properties for OME and heptane.

The FTIR calibration for OME was supplied by MKS Instruments. The concentration of OME was set to 562 ppm based on delivering 1.0 ml/h which could be dosed reliably and exactly through the syringe pump. Combining multiple fuel components in temperature-programmed oxidation experiments can result in a change of the light-off behavior. Therefore, OME was combined with CO and heptane.

3 Results and Discussion

T_{50} of a specific component is determined by using a conversion formula (1) which is applicable throughout the results. A conversion-temperature diagram was used to determine T_{50}. Experimental repetition showed an absolute error of 2 °C, which is applied to all T_{50} values.

Conversion formula for specific component:

$$Conversion\ of\ component\ X_i = \frac{x_{i,in} - x_{i,out}(T_{cat})}{x_{i,in}} * 100 \quad (1)$$

where $x_{i,in}$ is the initial recorded concentration of component i and $x_{i,out}$ is the recorded concentration of component i for specific temperature measured at the catalyst.

Table 1 Properties of OME and heptane

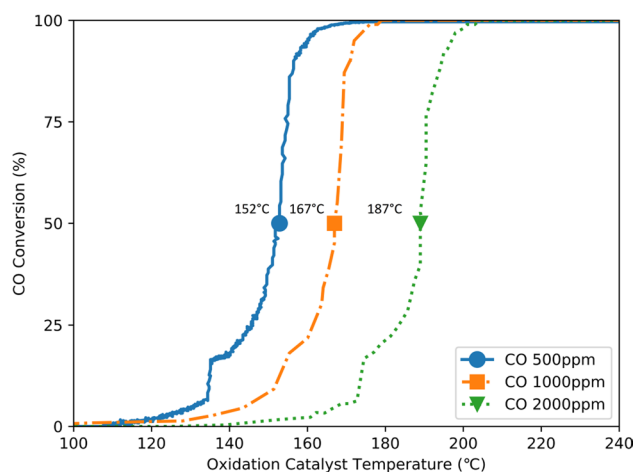|	OME	Heptane	Unit
Density (15 °C)	1.057	0.684 [24]	g cm^{-3}
Molar mass	150.7	100.2 [24]	g mol^{-1}
Stoichiometry	$C_{5.5}H_{13}O_{4.5}$	C_7H_{16}	-
Saturation vapor pressure $\log_{10}(P) = A - (B / (T + C))$	Dosed by evaporator with carrier gas	$A = 4.02832$ $B = 1268.636$ $C = -56.199$ [25]	-

Fig. 3 CO conversion in TPO experiments performed with three different CO concentrations in an exhaust gas comprising 10vol% O_2, 7.4vol% H_2O, and 7vol% CO_2 with GHSV of 60000 h^{-1} and a ramp of 5 °C per minute. The T_{50} oxidation temperatures of CO are given within the graph

Fig. 4 Heptane conversion in TPO experiments performed with three different C7 concentrations in an exhaust gas comprising of 10vol% O_2, 7.4vol% H_2O, and 7vol% CO_2 with GHSV of 60000 h^{-1} and a ramp of 5 °C per minute. The T_{50} oxidation temperatures of heptane are given in the graph

3.1 Light-off Experiments with CO

The results of experiments with three different CO concentrations of 500 ppm, 1000 ppm, and 2000 ppm are shown in Fig. 3, where the CO concentration is recorded by FTIR. With increasing temperature, more CO is converted to CO_2. $T_{50,CO}$ for 2000 ppm is determined to be approximately 187 °C, whereas for 1000 ppm and 500 ppm, it was determined to be 167 °C and 152 °C respectively. Hence, it can be concluded from these experiments that T_{50} increases noticeably with increasing CO concentration. At around 20% conversion of CO, there is a known concurrence between CO adsorption and CO oxidation with all three concentrations of CO. This can be explained by the CO inhibition effect, where the high concentration of CO at low temperature inhibits the rate of reaction, but once the reactant is gradually consumed, the concentration decreases and the conversion rate of CO to CO_2 increases [26]. At approximately 200 °C, the CO is reliably oxidized in all experiments. As higher temperatures are required to light-off the higher feed concentrations of CO, it can be described as self-inhibiting [19].

3.2 Light-off Experiments with Heptane

A set of comparable experiments are performed with heptane comprising three different input concentrations of 1000 ppm, 2000 ppm, and 3300 ppm. Such high concentrations exceed the regular engine exhaust in operation and are in general only reached by fuel dosing devices or late injection as part of a thermal management strategy for quick catalys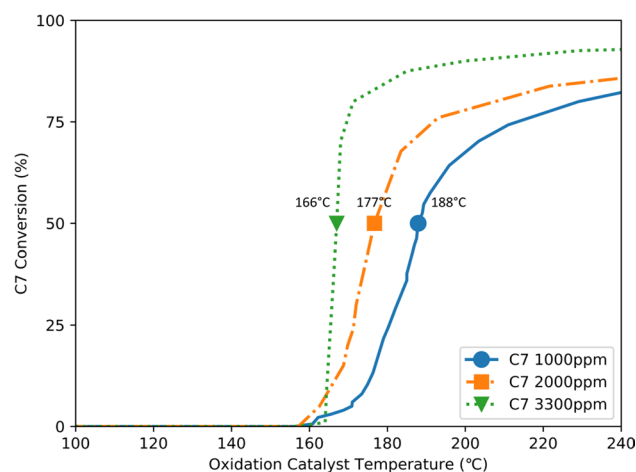t light-off. The resulting graph of heptane conversion measured over catalyst temperature is shown in Fig. 4. With an increase in concentration of heptane from 1000 to 3300 ppm, the measured $T_{50,C7}$ decreases from approximately 188 to 166 °C. A comparison of Figs. 3 and 4 clearly shows that the increasing heptane concentration has an opposite effect on T_{50} compared with the increasing CO concentration. The maximum conversion of 90% is observed and can be explained by a C_7 slip. One of the main reasons for the incomplete conversion of heptane can be identified as a high value of space velocity, which does not allow heptane to interact with the catalyst surface sufficiently for complete oxidation [20]. In the case of heptane and even more so for longer hydrocarbons, enough oxygen must be supplied for complete oxidation of species adsorbed at the catalyst surface.

3.3 Light-off Experiments for Heptane and CO Mixtures

To observe the effect of hydrocarbon oxidation and CO oxidation on each other, 1000 ppm of heptane and 1000 ppm of CO are mixed in the following experiment. The resulting graph is shown in Fig. 5 and compared to the test results in which only one of the components was dosed (see 1000 ppm from Figs. 3 and 4). While the light-off of CO is not influenced by the presence of heptane, $T_{50,C7}$ decreased from 188 to 172 °C. The oxidation of CO produces heat to activate heptane surface species enabling their oxidation. It can be concluded that CO addition can support the light-off of heptane (surrogate for diesel).
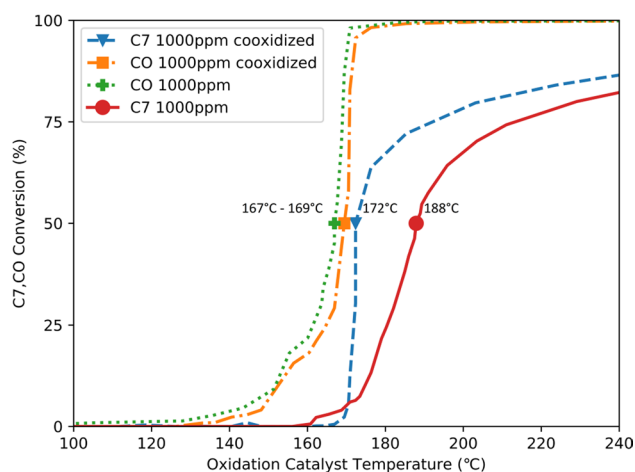
Fig. 5 C_7 and CO conversion in TPO experiments performed with a mixture of 1000 ppm of both components in an exhaust gas comprising 10vol% O_2, 7.4vol% H_2O, and 7vol% CO_2 with GHSV of 60000 h^{-1} and a ramp of 5 °C per minute and compared to the component itself. The T_{50} oxidation temperatures of CO and heptane are given in the graph

3.4 Light-off Experiments for CO and NO Mixtures

Figure 6 shows how $T_{50,CO}$ changes as incremental concentrations of NO are introduced in the exhaust gas mixture. The $T_{50,CO}$ of 1000 ppm CO is 167 °C. When 100 ppm of NO is introduced with 1000 ppm CO, the $T_{50,CO}$ increases to 196 °C. With 400 ppm NO, the $T_{50,CO}$ reaches a value of 209 °C. Thus, it can be concluded that NO significantly hinders CO conversion at temperatures between 150 and 210 °C. It can be expected that further increase in NO
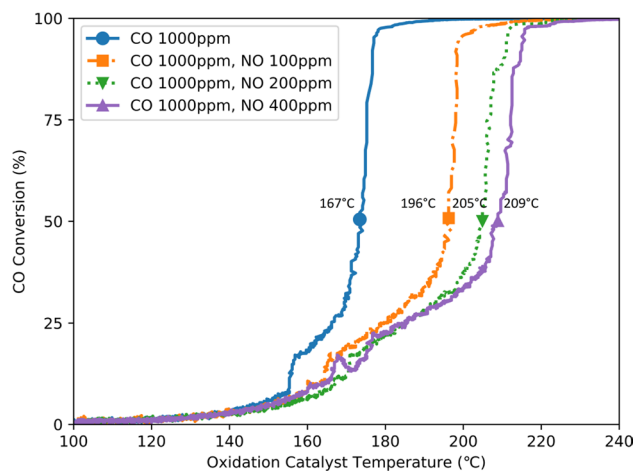

Fig. 6 CO conversion in TPO experiments performed with 1000 ppm CO and 100, 200, and 400 ppm of NO respectively in an exhaust gas comprising 10vol% O_2, 7.4vol% H_2O, and 7vol% CO_2 with GHSV of 60000 h^{-1} and a ramp of 5 °C per minute. The T_{50} oxidation temperatures of CO are given in the graph

concentration has a minor influence on $T_{50,CO}$ because the catalyst surface is saturated with NO.

The experiments were concluded once CO conversion was nearly complete. The conversion of NO to NO_2 could be detected by the FTIR measurement. In all experiments, a favorable ratio of NO to NO_2 of around 1:1 [27] was reached at a reaction temperature 230–240 °C, as shown in Fig. 7.

3.5 OME Oxidation Experiments

To better understand the light-off behavior of OME, experiments were performed with approximately 562 ppm of OME based on delivering 1.0 ml/h through the syringe pump. Since H_2O and CO_2 have disturbed the signal of OME and FA in the FTIR, the experiments were performed without CO_2 and H_2O [28].

All OME components were added up to an overall OME concentration, since the FTIR spectra of the single OME components hardly differ from each other. The main products detected via FTIR analysis in the TPO experiments with OME were FA, OME, and CO_2. The presence of FA was confirmed by an aqueous thymolphthalein solution positioned after the reactor. Within the solution, white polymeric solid deposits were found (see Fig. 8). As seen in Fig. 9, FA was detected already at 100 °C, due to the reactivity of OME at low temperatures over oxidation catalysts. The synthesis from methylal and trioxane is usually performed between 50 and 90 °C [29], which hints that OME is reactive at low temperatures with the presence of a catalyst. Without a catalyst FA is more stable, but water reacts readily with FA and its importance has been emphasized in many publications about OME synthesis [30]. At temperatures of around 200 °C, most of the introduced OME and build-up FA has
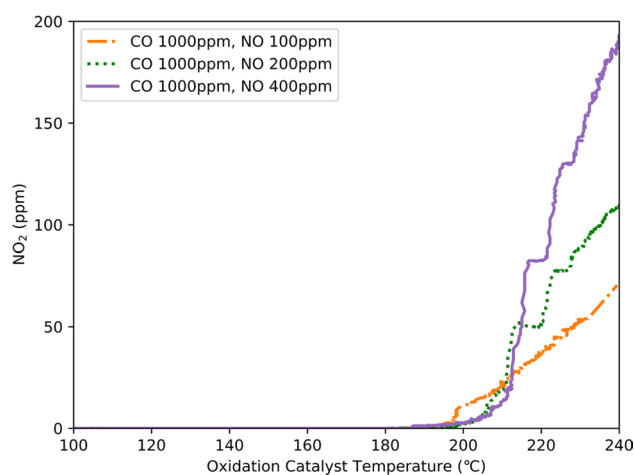

Fig. 7 NO_2 formation in TPO experiments performed with 1000 ppm CO and 100, 200, and 400 ppm of NO respectively in an exhaust gas comprising 10vol% O_2, 7.4vol% H_2O, and 7vol% CO_2 with GHSV of 60000 h^{-1} and a ramp of 5 °C per minute

Fig. 8 Picture of condensation bottles placed after the FTIR before the vent. To left bottle, the indicator thymolphthalein was added
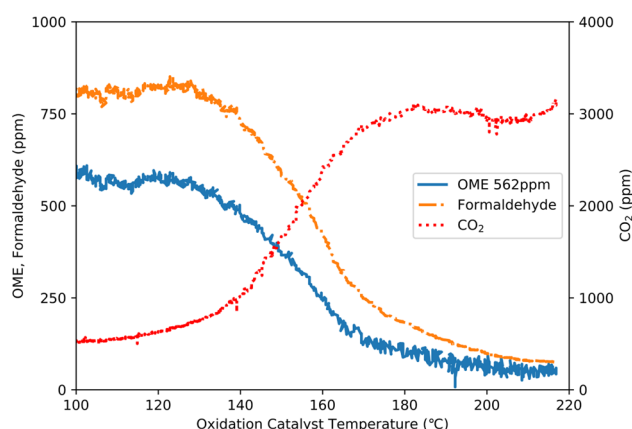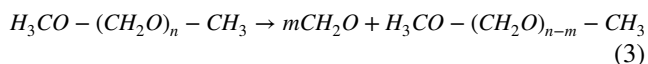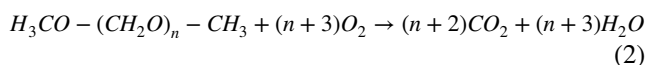

Fig. 9 OME oxidation in TPO experiments performed with 562 ppm OME in an exhaust gas comprising 10vol% O_2 (without H_2O and CO_2), GHSV of 60000 h^{-1}, and a ramp of 5 °C per minute

oxidized to CO_2 at the catalyst. The conversion of OME to FA and consequently to CO_2 can be described as shown in Eqs. (2) and (3):

$$H_3CO - (CH_2O)_n - CH_3 + (n+3)O_2 \rightarrow (n+2)CO_2 + (n+3)H_2O \tag{2}$$

$$H_3CO - (CH_2O)_n - CH_3 \rightarrow mCH_2O + H_3CO - (CH_2O)_{n-m} - CH_3 \tag{3}$$

The starting heating temperature of the experiment was 100 °C. This was held more than 5 min until the signals of FA, CO_2, and OME were stable. Approximately 500 ppm CO_2 (200 ppm from air and 300 ppm from OME oxidation) was measured at the starting temperature. According to the C-balance from the OME conversion Eqs. (2) and (3), 3090 ppm of CO_2 was expected upon complete oxidation, which is roughly equivalent to what was obtained in the experiment as shown in Fig. 9. At 220 °C, approximately 3000 ppm CO_2 was recorded, where 200 ppm is received from the air input content and approximately 2800 ppm of CO_2 received from OME and FA oxidation. The missing

carbon species can be found in the remaining OME and FA signal, since both are not completely oxidized at 220 °C.

Even though the intermediate steps of OME oxidation are still unclear, it was possible to determine $T_{50,OME}$ in this experiment. Figure 10 shows the conversion of OME and FA over the oxidation catalyst and $T_{50,OME}$ and $T_{50,FA}$ are determined to be 156 °C and 161 °C respectively. This correlates with the literature values for T_{50} of aldehydes, which are between 145 and 160 °C [31], as could be expected due to their similar structures.

3.6 Light-off Experiments for OME and Heptane Mixtures

A light-off experiment with 1000 ppm heptane was compared with a mixture of 1000 ppm heptane and 562 ppm OME to observe the effect of OME on the oxidation of heptane. It was evident from $T_{50,C7}$ that OME has no significant influence on the oxidation of heptane. As seen in Fig. 11, the addition of OME resulted in a temperature reduction of 5 °C in $T_{50,C7}$. The heat of reaction from the oxidation of OME is therefore measurable but not sufficient to majorly support heptane oxidation at lower temperatures. More OME could be used in relation to heptane to increase the impact, as seen in the experiment with 1000 ppm CO and 1000 ppm heptane. With CO, the oxidation curve was a lot steeper at conversions between 0 and 50%.

3.7 Light-off Experiments for OME and CO Mixtures

To analyze the influence of OME on $T_{50,CO}$, an experiment with 1000 ppm CO and 562 ppm OME was performed and
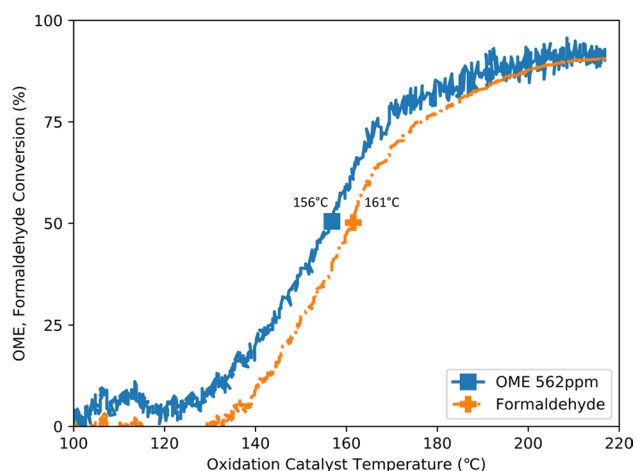

Fig. 10 OME conversion in TPO experiments performed with 562 ppm OME in an exhaust gas comprising 10vol% O_2 (without H_2O and CO_2), GHSV of 60000 h^{-1}, and a ramp of 5 °C per minute. The T_{50} oxidation temperatures of OME and FA are given in the graph
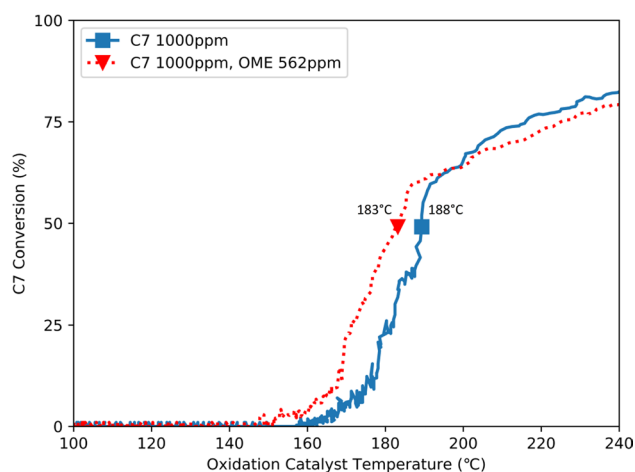
Fig. 11 Heptane conversion in TPO experiments performed with 1000 ppm C_7 and with a mixture of 1000 ppm C_7 and 562 ppm OME in an exhaust gas comprising 10vol% O_2, 7.4vol% H_2O, and 7vol% CO_2 with GHSV of 60000 h^{-1} and a ramp of 5 °C per minute. The T_{50} oxidation temperatures of heptane are given within the graph

compared with the experiment carried out with only CO. Figure 12 shows that $T_{50,CO}$ increases from approximately 167 to 183 °C with the addition of 562 ppm OME. The adverse effect of OME on the $T_{50,CO}$ is opposite to what was observed earlier in Fig. 11, where OME has a slightly positive effect on the $T_{50,C7}$. Furthermore, the shape of the CO conversion curve changes as the gradient is a lot lower. Especially at conversions over 50% CO, the influence of the OME input is evident. A concurrence between CO and OME conversion on the surface can be concluded. Products
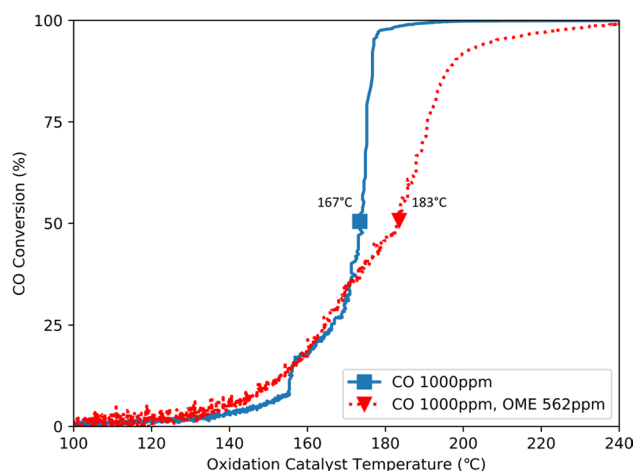
formed from OME, like FA or surface species, could be the main reason for this.

3.8 Light-off Experiments for OME and NO Mixtures

To observe the effect of NO on $T_{50,OME}$, two more experiments were carried out with the combination of 562 ppm of OME and 100 and 400 ppm of NO respectively. Similar experiments were performed with CO, which showed an increase in $T_{50,CO}$ with an increase in NO concentration (Fig. 6). In the case of OME with NO, the results were comparable as the addition of NO was shown to have an increasing effect on $T_{50,OME}$. This result is similar to CO, as shown in Fig. 12.

The shown signals of OME with NO were achieved by plotting the moving averages on the order 10, since the FTIR spectra showed a lot of noise. However, it can be observed that the $T_{50,OME}$ increases from 156 to 177 °C after addition of 100 ppm NO and finally to 185 °C with 400 ppm NO (Fig. 13).

4 Conclusion

Light-off experiments were performed with CO, heptane, and OME in order to identify the corresponding T_{50}, while also analyzing the effect on T_{50} by varying parameters such as concentration and mixing with other exhaust gas components.

$T_{50,CO}$ increases with increasing CO concentration. With heptane, the opposite effect is observed as $T_{50,C7}$ decreases with increasing concentration. When a mixture of CO and
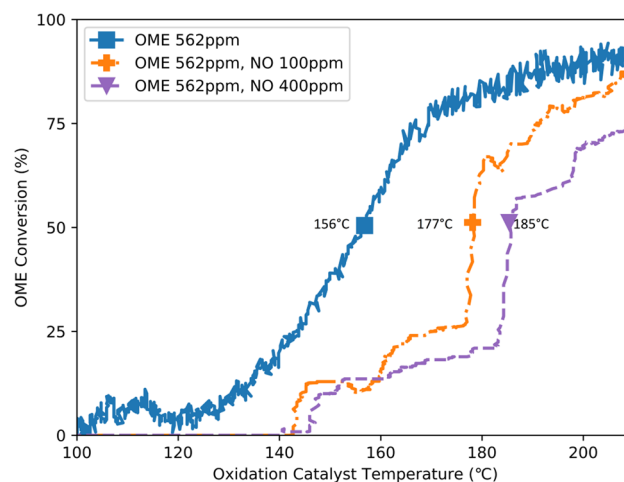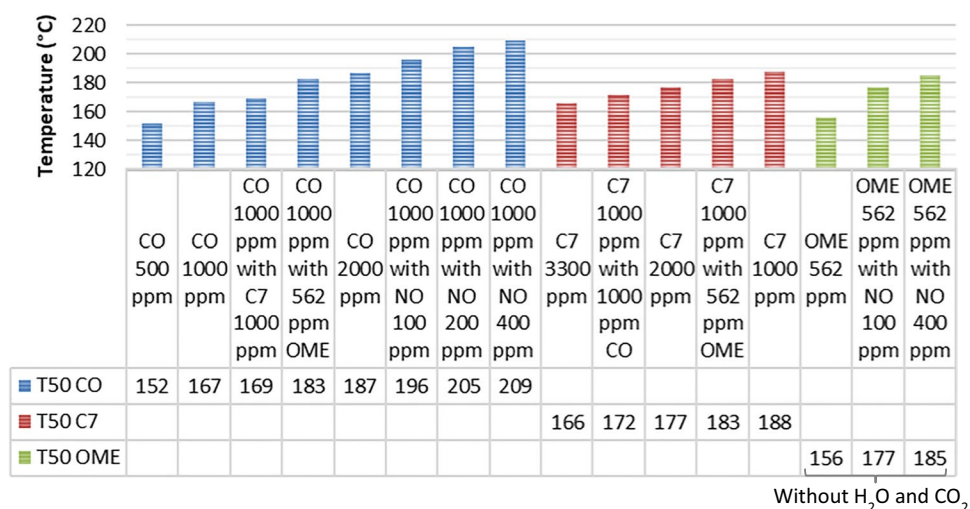

Fig. 12 CO conversion in TPO experiments performed with 1000 ppm CO and a mixture of 1000 ppm CO with 562 ppm OME in an exhaust gas comprising 10vol% O2, 7.4vol% H2O, and 7vol% CO2 with GHSV of 60000 h^{-1} and a ramp of 5 °C per minute. The T_{50} oxidation temperatures of CO are given in the graph

Fig. 13 OME conversion in TPO experiments performed with 562 ppm of OME and 100 and 400 ppm of NO respectively in an exhaust gas comprising 10vol% O_2 (without H_2O and CO_2), GHSV of 60000 h^{-1}, and a ramp of 5 °C per minute. The T_{50} oxidation temperatures of OME are given in the graph

Table 2 Results overview T_{50}

	CO 500 ppm	CO 1000 ppm	CO 1000 ppm with C7 1000 ppm	CO 1000 ppm with 562 ppm OME	CO 2000 ppm	CO 1000 ppm with NO 100 ppm	CO 1000 ppm with NO 200 ppm	CO 1000 ppm with NO 400 ppm	C7 3300 ppm	C7 1000 ppm with 1000 ppm CO	C7 2000 ppm	C7 1000 ppm with 562 ppm OME	C7 1000 ppm	OME 562 ppm	OME 562 ppm with NO 100 ppm	OME 562 ppm with NO 400 ppm
T50 CO	152	167	169	183	187	196	205	209								
T50 C7									166	172	177	183	188			
T50 OME														156	177	185

Without H_2O and CO_2

heptane is oxidized, CO reduces $T_{50,C7}$ whereas the $T_{50,CO}$ is unaffected by the presence of heptane. Table 2, which includes all experiments presented in this paper, is added to simplify a comparison.

In oxidation experiments with OME, FA already started to build at temperatures of 100 °C leveling to an equilibrium concentration, which remained constant until 130 °C. This behavior is not known from conventional hydrocarbon fuels and was not found in heptane experiments, since the C–C bonds are more stable against catalytic splitting. The C–O bond of OME is more willing to build a C=O double bond than the C–O bond of gaseous CO, as no FA is detected in CO oxidation experiments. In engine experiments with oxygenated fuel, FA was also found in the exhaust gas [17, 32].

For 562 ppm OME used in the light-off experiments presented here, $T_{50,OME}$ and $T_{50,FA}$ are identified as 156 °C and 161 °C respectively. When analyzing the effect of OME on $T_{50,C7}$ and $T_{50,CO}$ through mixture experiments, contrasting results were obtained. In the case of CO, $T_{50,CO}$ increased with the introduction of OME. This agrees with the other CO experiments mentioned before as $T_{50,CO}$ increased with the increasing CO concentration. This can be explained by the fact that both molecules having C–O bonds probably build similar surface species on the catalyst. The production of FA could also play a major role in blocking the catalyst surface.

However, when OME is mixed with heptane, $T_{50,C7}$ decreases. The known effect of NO hindering oxidation by blocking the catalyst surface and its impact on $T_{50,C7}$ was verified with OME. The impact of OME reducing $T_{50,C7}$ in a mixture with heptane is small; however, it is interesting considering the easy miscibility of the two fuels and the prospect of diesel and OME being used together as a blend in ICEs. The high reactivity of OME at low temperatures is useful for exhaust after-treatment catalysts in cold start conditions.

In general, combustion and exhaust after-treatment development must proceed together. Due to the high cetane number of OME, an engine designed for OME combustion with high compression ratios could probably further reduce not only soot but also hydrocarbons and carbon monoxide. At the same time, during experimentation, secondary products like FA and nitrous oxide must be analyzed in terms of toxicity and methane for the determination of the greenhouse potential. FA analysis is especially relevant at low temperatures, because when the engine load increases, FA emissions decrease [32]. At stoichiometric combustion, OME produces more water compared to diesel at the same load point. Adapted light-off investigations should be performed, when OME combustion is set and the product gases and their dynamic occurrence are known better.

To enable and establish OME in ICEs, it is important that the oxidation catalyst rapidly reaches the temperature levels above 160 °C quickly. External catalyst heating measures will gain importance with OME blending in order to suppress the significant emission of FA and ensuring full oxidation. Otherwise, thermal management measures will be severely limited. One solution could be a technology called CatVap®, developed and presented from Fraunhofer ISE, which provides chemical heating power while changing the fuel composition to components with low T_{50} oxidation temperatures, like ethene and propene [33, 34]. The light-off behavior of the mixture provided by the CatVap® system is further investigated in the C3 Mobility project.

Data Availability Not applicable

Code Availability Not applicable

Declarations

Conflict of Interest The authors declare that they have no competing interests.

References

1. Thiruvengadam, A., Delgado, O.: Heavy-Duty Vehicle Diesel Engine Efficiency Evaluation and Energy Audit (2014) The International Council on Clean Transportation. https://theicct.org/sites/default/files/publications/HDV_engine-efficiency-eval_WVU-rpt_oct2014.pdf

2. Luján, J.M., Climent, H., Ruiz, S., Moratal, A.: Influence of ambient temperature on diesel engine raw pollutants and fuel consumption in different driving cycles. Int. J. Engine Res. (2019). https://doi.org/10.1177/1468087418792353

3. Bai, S., Han, J., Liu, M., Qin, S., Wang, G., Li, G.: Experimental investigation of exhaust thermal management on NOx emissions of heavy-duty diesel engine under the World Harmonized transient Cycle (WHTC). Appl. Therm. Eng. (2018). https://doi.org/10.1016/j.applthermaleng.2018.07.042

4. Demuynck, J., Favre, C., Bosteels, D., Bunar, F., Spitta, J., Kuhrt, A.: Diesel vehicle with ultra-low NOx emissions on the road. In: SAE Technical Paper Series. 14th International Conference on Engines & Vehicles, SEP. 15, 2019. SAE International400 Commonwealth Drive, Warrendale, PA, United States (2019). https://doi.org/10.4271/2019-24-0145

5. Kovacs, D., Rauch, H., Rezaei, R., Huang, Y., Harris, T.: Modeling heavy-duty engine thermal management technologies to meet future cold start requirements. In: SAE Technical Paper Series. WCX SAE World Congress Experience, APR. 09, 2019. SAE International400 Commonwealth Drive, Warrendale, PA, United States (2019). https://doi.org/10.4271/2019-01-0731

6. Demuynck, J., Bosteels, D., Bunar, F., Spitta, J.: Diesel-Pkw mit extrem niedrigem NOx-Niveau im Realfahrbetrieb. MTZ Motortech Z (2020). https://doi.org/10.1007/s35146-019-0157-4

7. Boutikos, P., Žák, A., Kočí, P.: CO and hydrocarbon light-off inhibition by pre-adsorbed NOx on Pt/CeO2/Al2O3 and Pd/CeO2/Al2O3 diesel oxidation catalysts. Chem. Eng. Sci. (2019). https://doi.org/10.1016/j.ces.2019.115201

8. Rößler, M., Velji, A., Janzer, C., Koch, T., Olzmann, M.: Formation of engine internal NO 2: measures to control the NO 2/NO X ratio for enhanced exhaust after treatment. SAE Int. J. Engines (2017). https://doi.org/10.4271/2017-01-1017

9. Brandt, E.P., Wang, Y., Grizzle, J.W.: Dynamic modeling of a three-way catalyst for SI engine exhaust emission control. IEEE Trans. Contr. Syst. Technol. (2000). https://doi.org/10.1109/87.865850

10. Baranowski, C.J., Bahmanpour, A.M., Kröcher, O.: Catalytic synthesis of polyoxymethylene dimethyl ethers (OME): a review. Appl. Catal. B (2017). https://doi.org/10.1016/j.apcatb.2017.06.007

11. Hank, C., Lazar, L., Mantei, F., Ouda, M., White, R.J., Smolinka, T., Schaadt, A., Hebling, C., Henning, H.-M.: Comparative well-to-wheel life cycle assessment of OME 3–5 synfuel production via the power-to-liquid pathway. Sustainable Energy Fuels (2019). https://doi.org/10.1039/C9SE00658C

12. Salem, M.K.O.: New Routes for Efficient and Sustainable Oxymethylene Ethers Synthesis. Universitätsbibliothek der TU München, München (2020)

13. Härtl, M., Gaukel, K., Pélerin, D., Wachtmeister, G.: Oxymethylenether als potenziell CO2-neutraler Kraftstoff für saubere Dieselmotoren Teil 1. Motorenuntersuchungen. MTZ Motortech Z (2017). https://doi.org/10.1007/s35146-016-0170-9

14. Omari, A., Heuser, B., Wiartalla, A., Bergmann, D.: Stromgenerierte Kraftstoffe für mobile Maschinen. ATZ Offhighway (2018). https://doi.org/10.1007/s35746-018-0016-0

15. Willems, Werner (W.), Dr.-Ing. Jost Weber, Dr.-Ing. Olaf Erik Herrmann (eds.): DME/OME1 -Nachhaltige Kraftstoffe für den selbstzündenden Verbrennungsmotor für Pkw und Nutzfahrzeuganwendungen (2019)

16. Jacob, E., Maus, W.: Oxymethylenether als potenziell CO2-neutraler Kraftstoff für saubere Dieselmotoren Teil 2. Erfüllung des Nachhaltigkeitsanspruchs. MTZ Motortech Z (2017). https://doi.org/10.1007/s35146-017-0017-z

17. Pélerin, D., Gaukel, K., Härtl, M., Jacob, E., Wachtmeister, G.: Potentials to simplify the engine system using the alternative diesel fuels oxymethylene ether OME1 and OME3−6 on a heavy-duty engine. Fuel (2020). https://doi.org/10.1016/j.fuel.2019.116231

18. Ye, S., Yap, Y.H., Kolaczkowski, S.T., Robinson, K., Lukyanov, D.: Catalyst 'light-off' experiments on a diesel oxidation catalyst connected to a diesel engine—methodology and techniques. Chem. Eng. Res. Des. (2012). https://doi.org/10.1016/j.cherd.2011.10.003

19. Mathieu, O., Lavy, J., Jeudy, E.: Investigation of hydrocarbons conversion over a Pt-based automotive diesel oxidation catalyst: application to exhaust port fuel injection. Top Catal (2009). https://doi.org/10.1007/s11244-009-9365-3

20. Arve, K., Klingstedt, F., Eranen, K., Warna, J., Lindfors, L., Murzin, D.: Kinetics of NO reduction over Ag/alumina by higher hydrocarbon in excess of oxygen, vol. 107 (2005)

21. Wiebenga, M.H., Oh, S.H., Qi, G.: Cold-start emission reduction potential and limitations of commercial passive hydrocarbon adsorbers. Emiss. Control Sci. Technol. (2017). https://doi.org/10.1007/s40825-016-0052-0

22. Likhanov, V.A., Lopatin, O.P.: Study of toxicity of diesel engine on alcohol fuel. IOP Conf. Ser.: Earth Environ. Sci (2020). https://doi.org/10.1088/1755-1315/421/7/072018

23. Ouda, M., Mantei, F.K., Elmehlawy, M., White, R.J., Klein, H., Fateen, S.-E.K.: Describing oxymethylene ether synthesis based on the application of non-stoichiomsetric Gibbs minimisation. React. Chem. Eng. (2018). https://doi.org/10.1039/C8RE00006A

24. PubChem: CID 8900, Heptane. https://doi.org/10.5517/cc3gcqm

25. Willingham, C.B., Taylor, W.J., Pignocco, J.M., Rossini, F.D.: Vapor pressures and boiling points of some paraffin, alkylcyclopentane, alkylcyclohexane, and alkylbenzene hydrocarbons. J. Res. Natl. Bur. Stan. (1945). https://doi.org/10.6028/jres.035.009

26. Stephen Salomons: Kinetic Models for a Diesel Oxidation Catalyst. Thesis for PhD, University of Alberta (2007). https://www.researchgate.net/publication/221677425_Kinetic_Models_for_a_Diesel_Oxidation_Catalyst

27. Ciardelli, C., Nova, I., Tronconi, E., Chatterjee, D., Bandl-Konrad, B., Weibel, M., Krutzsch, B.: Reactivity of NO/NO2–NH3 SCR system for diesel exhaust aftertreatment: identification of the reaction network as a function of temperature and NO2 feed content. Appl. Catal. B (2007). https://doi.org/10.1016/j.apcatb.2005.10.041

28. Univ.-Prof. Dr.-Ing. Roland Baar Univ.-Prof. Dr.-Ing. Michael Bargende Univ.-Prof. Dr. techn. Christian Beidl Univ.-Prof. Dr. sc. techn. Thomas Koch Univ.-Prof. Dr.-Ing. Hermann Rottengruber: Wissenschaftliche Untersuchungen hardwareseitiger NOX-Reduzierungsnachrüstmöglichkeiten im Pkw-Bereich und im Segment der leichten Nutzfahrzeuge (2018)

29. Burger, J., Ströfer, E., Hasse, H.: Chemical equilibrium and reaction kinetics of the heterogeneously catalyzed formation of poly(oxymethylene) dimethyl ethers from methylal and trioxane. Ind. Eng. Chem. Res. (2012). https://doi.org/10.1021/ie301490q

30. Baranowski, C.J., Fovanna, T., Roger, M., Signorile, M., McCaig, J., Bahmanpour, A.M., Ferri, D., Kröcher, O.: Water inhibition of oxymethylene dimethyl ether synthesis over zeolite H-beta: a combined kinetic and in situ ATR-IR study. ACS Catal. (2020). https://doi.org/10.1021/acscatal.0c01805

31. Diehl, F.: OXYDATION CATALYTIQUE TOTALE DES HYDROCARBURES LOURDS SUR Pt/Al2O3 (1998). https://www.researchgate.net/publication/278827913_OXYDATION_CATALYTIQUE_TOTALE_DES_HYDROCARBURES_LOURDS_SUR_PtAl2O3

32. Notheis, D., Wagner, U., Velji, A., Koch, T.: Formation of nitrogen dioxide and formaldehyde in a medium duty diesel engine with oxygenated fuels. In: ASME 2020 Internal Combustion Engine. https://doi.org/10.1115/ICEF2020-2923

33. Szolak, R.: CatVap® – Abgasnachbehandlungssysteme der Zukunft benötigen effiziente Heizmaßnahmen. Internationales AVL Forum Abgas- und Partikelemissionen, 3 March 2020

34. Szolak, R.: CatVap® – neue Aufheizmaßnahme für Abgasnachbehandlungssysteme. Heavy-Duty-, On- und Off-Highway-Motoren, Friedrichshafen, 27 November 2019